Fast-Neutron Scattering from Ta, Re, and Pt*

A. B. SMITH, P. T. GUENTHER, AND J. F. WHALEN
Argonne National Laboratory, Argonne, Illinois
(Received 27 November 1967)

The scattering of neutrons with energies of $\lesssim$1.5 MeV from the elements Ta, Re, and Pt was experimentally studied. Elastic and inelastic neutron-scattering angular distributions were determined at incident-neutron-energy intervals of $\lesssim$20 keV throughout the range 0.3 to 1.5 MeV. Time-of-flight measurements were made concurrently at eight or more scattering angles between 25° and 155° with sufficient scattered-neutron-energy resolution to separate the elastically scattered component from most inelastically scattered neutron groups. Differential inelastic scattering cross sections corresponding to the excitation of the following states were observed: in Ta at 144±10 (doublet), 313±15, 506±20, 620±20, 720±20, and 930±25 keV; in Re at 132±10, 219±15, 313±15, 387±18, 518±20, 637±20, 767±25, 865±25, 963±25, 1060±25, and 1135±25 keV; and in Pt at 130±20, 214±20, 348±15, 420±15, 620±20, 719±15, 838±25, and 935±20 keV. The experimental results were compared with calculations based upon the optical model and the Hauser-Feshbach formula including corrections for resonance-width fluctuations. The experimentally observed level structure is discussed in the context of single-particle and rotational states of deformed nuclei.

I. INTRODUCTORY REMARKS

THE study of fast neutron scattering from heavy nuclei can provide an insight into the validity of the optical model and statistical concepts in regions of appreciable deformation, free from the complexities of Coulomb effects. Calculation of neutron scattering using deformed potentials is difficult, particularly for odd-A nuclei, and thus it is desirable to determine to what extent a spherical potential approximation is valid. With the latter objective, it is useful to examine neutron scattering from nuclei of similar masses but large and differing deformations. The elements Ta, Re, and Pt consist of such nuclei. They are similar in mass and charge, but vary in deformation δ from $\sim$0.3 (Ta) to $\sim$0.15 (Pt).[1] Previous experimental studies of neutron scattering from these elements have been largely confined to a few incident neutron energies and/or have provided little knowledge of the inelastically scattered neutron spectrum.[2–11] Because of this limited experimental base, quantitative comparison with calculation has been difficult.[12–19]

The low-energy excited structures of Ta, Re, and Pt are characterized by collective rotational-vibrational and single-particle states.[20] A wealth of structure information pertinent to these elements has been reported, particularly as the result of radioactive decay and Coulomb excitation studies.[21–24] Despite this fund of knowledge, there remain significant discrepancies between the structure reported from experiment and the theoretical predictions.

The present experiments attempt to provide quantitative knowledge of fast neutron scattering from Ta, Re, and Pt of such quality and scope as to form a foundation for the development of calculational methods and assay of their validity. The measured values are used to determine spherical optical potentials which, together with compound nucleus theory, provide calculated cross sections in quantitative agreement with experiment, permit the extrapolation and interpolation of measured values, and furnish a mechanism for correlating observed and theoretically predicted excited nuclear structure. It is an intent to contribute to the understanding of the structure of the isotopes of Ta, Re, and Pt, particularly those facets best studied through the observation of low-energy inelastic neutron scattering. In addition, the experimental results are of extensive value in applied nuclear-energy programs, as

* This work supported by the U. S. Atomic Energy Commission.
1 P. Stelson and L. Grodzins, Nucl. Data **1A**, 21 (1965–1966).
2 A. Langsdorf, R. Lane, and J. Monahan, Argonne National Laboratory Report No. ANL-5567 (Rev.), 1961 (unpublished); see also, R. Lane *et al.*, Ann. Phys. (N. Y.) **12**, 135 (1961).
3 M. Walt and H. Barschall, Phys. Rev. **93**, 1062 (1964).
4 A. B. Smith, Argonne National Laboratory Report No. ANL-6726, 1963 (unpublished).
5 J. Beyster *et al.*, Phys. Rev. **104**, 1319 (1956).
6 J. Guernsey and A. Wattenburg, Phys. Rev. **101**, 1516 (1956).
7 D. I. Garber and E. F. Shrader, Bull. Am. Phys. Soc. **6**, 61 (1961).
8 W. B. Gilboy and J. H. Towle, Nucl. Phys. **42**, 86 (1963).
9 R. B. Day, Phys. Rev. **102**, 767 (1956).
10 D. A. Lind and R. B. Day, Ann. Phys. (N. Y.) **12**, 485 (1961).
11 Brookhaven National Laboratory Report No. BNL-400, edited by M. Goldberg *et al.* 2nd ed., Vol. II, 1962 (unpublished).
12 F. Perey and B. Buck, Nucl. Phys. **32**, 353 (1962).
13 D. Chase *et al.*, Phys. Rev. **110**, 1080 (1958).
14 R. N. Maddison, Nucl. Phys. **54**, 417 (1964).
15 E. Auerbach and S. Moore, Phys. Rev. **135**, B895 (1964).
16 L. Rosen, Los Alamos Scientific Laboratory Report No. LA-3538, 1966 (unpublished); see also, L. Rosen, in *Proceedings of the International Conference on the Study of Nuclear Structure with Neutrons* (North-Holland Publishing Co., Amsterdam, 1966), p. 379.
17 F. Perey, in *Proceedings of the International Conference on the Study of Nuclear Structure with Neutrons* (North-Holland Publishing Co., Amsterdam, 1966), p. 418.
18 P. E. Hodgson, *The Optical Model of Elastic Scattering* (Oxford University Press, London, 1963).
19 S. Moore and E. Auerbach, Brookhaven National Laboratory Report No. BNL-818, 1963 (unpublished); see also Ref. 15.
20 B. R. Mottelson and S. G. Nilsson, Kgl. Danske Videnskab. Selskab, Mat. Fys. Skrifter **1**, No. 8 (1959).
21 *Nuclear Data Sheets*, compiled by K. Way *et al.*, (U. S. Government Printing Office, National Academy of Sciences—National Research Council, Washington, D. C.), NRC 60-2-111.
22 P. Stelson and F. McGowan, Phys. Rev. **99**, 112 (1955); **109**, 109 (1958).
23 K. Y. Chu and M. L. Wiedenbeck, Phys. Rev. **75**, 226 (1949).

Ta and Re are structural materials with excellent high-temperature properties.

II. EXPERIMENTAL METHOD

The neutron-scattering measurements were carried out with an automated multiangle time-of-flight system and an associated pulsed and bunched Van de Graaff accelerator. This laboratory system, its use, and the associated data handling procedures have been described in detail; thus the apparatus and method will only be outlined here.[25]

The positive-ion pulsed Van de Graaff and associated magnetic bunching system was capable of producing ~1-nsec proton bursts with peak intensities of $\lesssim 10$ mA.[26,27] The proton bursts were converted into essentially monoenergetic neutron bursts by means of the $Li^7(p,n)Be^7$ source reaction.[28] The neutron-scattering samples were fabricated from the natural metal in the form of right cylinders measuring 2 cm in length and 2 cm in diameter of 1.8 cm in diameter and 1.8 cm in length. These samples were placed ~10 cm from the neutron source at a zero-degree source-reaction angle. The sample-source geometry and the lithium source-target thicknesses were arranged to provide incident-neutron-energy spreads at the scattering samples of 10 to 30 keV. The choice of incident-neutron-energy definition was dictated by the objectives of the particular measurement. Scattered neutron time spectra were determined concurrently in eight or more detectors placed 2 to 3 m from the scattering samples. The detectors were distributed over laboratory scattering angles between 25° and 155°. Neutron source intensities were monitored with a number of "long counters" placed at various reaction angles, including zero degrees.[29]

The apparatus provided a scattered neutron sensitivity of a few millibarns per steradian and a scattered neutron-energy resolution $\gtrsim 15$ keV. Time spectra selected from a large number of measurements are shown in Fig. 1. These results are illustrative of those used in determinations of elastic and inelastic scattering angular distributions and respective differential cross sections.

All measured cross sections were determined relative to the known elastic scattering cross sections of carbon.[2] The experimental information was sufficiently processed, on-line, using a digital computer to ensure a reasonable quality of the data. Subsequent off-line data processing included reduction of observed time spectra to cross sections, corrections for incident beam attenuation and multiple scattering within the samples, and corrections for scattered neutron angular resolution.[25] The final corrected cross sections were available in numerical and graphical form.

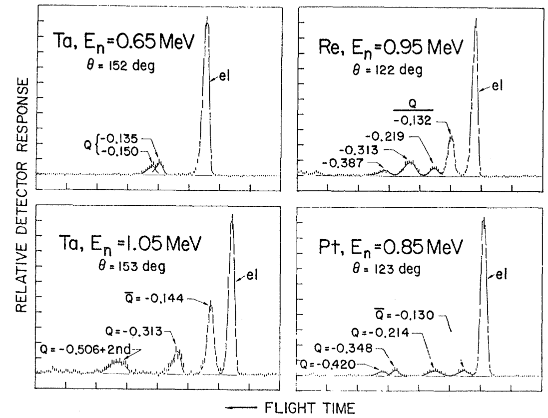

FIG. 1. Time spectra obtained by scattering neutrons from Ta, Re, and Pt. Time per channel was ~1.05 nsec and flight path ~2.0 m. Q values are indicated in MeV. Small backgrounds have been subtracted and all spectra normalized to the same elastic peak height. No detector sensitivity corrections have been applied and detector biases were chosen to emphasize the resolution of scattering resulting in the excitation of low-lying states. The vertical bars indicate the statistical standard deviations of the respective measurements.

Where total cross-section values reported in the literature were found in qualitative disagreement with the cumulative sums of elastic and inelastic scattering results of this work (Ta) or in those cases where reported total cross sections were sparse (Re) direct measurements of total cross sections were undertaken. These were transmission measurements employing the $Li^7(p,n)Be^7$ reaction as a neutron source.[30] The lithium targets and the experimental geometries were arranged so as to provide the desired neutron resolutions. Neutron detection was accomplished either with liquid scintillators employing pulse-shape discrimination for γ-ray rejection or with a shielded battery of BF_3 proportional counters. The measurements were carried out in a fully automatic manner using a digital computer for on-line data acquisition and reduction, and feed-back control to the nuclear accelerator, sample changer, and other portions of the apparatus.[31]

III. EXPERIMENTAL RESULTS

A. Elastic Scattering

Differential elastic neutron-scattering cross-section measurements were not always made with identical scattering angles but the angles were accurately determined for each experimental arrangement. Measurements were made at $\lesssim 20$-keV incident-neutron-energy intervals from 0.3 to 1.5 MeV with incident-neutron-

[24] B. Burson *et al.*, Phys. Rev. **87**, 252 (1951).
[25] A. B. Smith *et al.*, Nucl. Instr. Methods **50**, 277 (1967).
[26] R. C. Mobley, Phys. Rev. **88**, 360 (1952).
[27] L. Cranberg *et al.*, Nucl. Instr. Methods **12**, 335 (1961).
[28] H. Newson and J. Gibbons, in *Fast Neutron Physics*, edited by J. Marion and J. Fowler (Interscience Publishers, Inc., New York, 1960), Vol. I, p. 133.
[29] A. O. Hanson and J. L. McKibbon, Phys. Rev. **72**, 673 (1947).
[30] D. Miller, in *Fast Neutron Physics*, edited by J. Marion and J. Fowler (Interscience Publishers, Inc., New York, 1960), Part II, p. 985.
[31] J. F. Whalen *et al.*, Nucl. Instr. Methods **39**, 185 (1966).

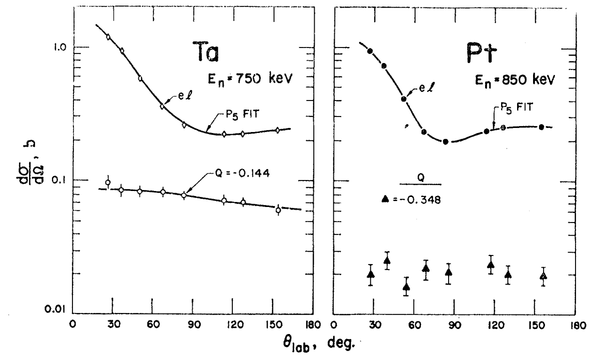

FIG. 2. Differential elastic and inelastic cross sections for the scattering of 750-keV neutrons from Ta (left) and 850-keV neutrons from Pt (right). The measured elastic values are compared with the least-squares fit of Eq. (1) to the data. Measured inelastic cross sections for the excitation of the *144*-keV state in Ta and the *348*-keV state in Pt are indicated.

energy resolutions of ~20 keV. At incident neutron energies of $\lesssim$1.2 MeV the elastically scattered neutrons were resolved from essentially all inelastic contributions (see Fig. 1 for illustration). An exception was scattering from Ta, where inelastic processes resulting in the excitation of the first state at ~6 keV were not resolved from the elastic contribution.[21] At incident neutron energies >1.2 MeV, it was occasionally necessary to correct the observed elastic scattering results for contributions from inelastic scattering, leaving the residual nucleus in the first excited state. These corrections were determined from careful measurements at incident energies >1.2 MeV, employing particularly long (3 to 4 m) flight paths and a limited number of scattering angles. Where necessary these corrections were based upon calculational extrapolation of the measured inelastic scattering results (see Sec. IV below).

The experimental differential elastic scattering cross sections were expressed as Legendre expansions of the form

$$\frac{d\sigma}{d\Omega}=\frac{\sigma}{4\pi}\left[1+\sum_{i=1}^{5}\omega_i P_i\right], \qquad (1)$$

where σ is the elastic scattering cross section, ω_i are coefficients of the expansion of the angular distributions in terms of Legendre polynomials P_i, and all angles are expressed in the laboratory system. ω_i and σ values were obtained from a least-squares fit of Eq. (1) to the measured distributions. Expressed in the form of Eq. (1), the results were representative of the actual measured differential elastic cross sections, as illustrated in Fig. 2, and permitted easy comparison of measurements made with slightly different experimental configurations, particularly scattering angles. Results in

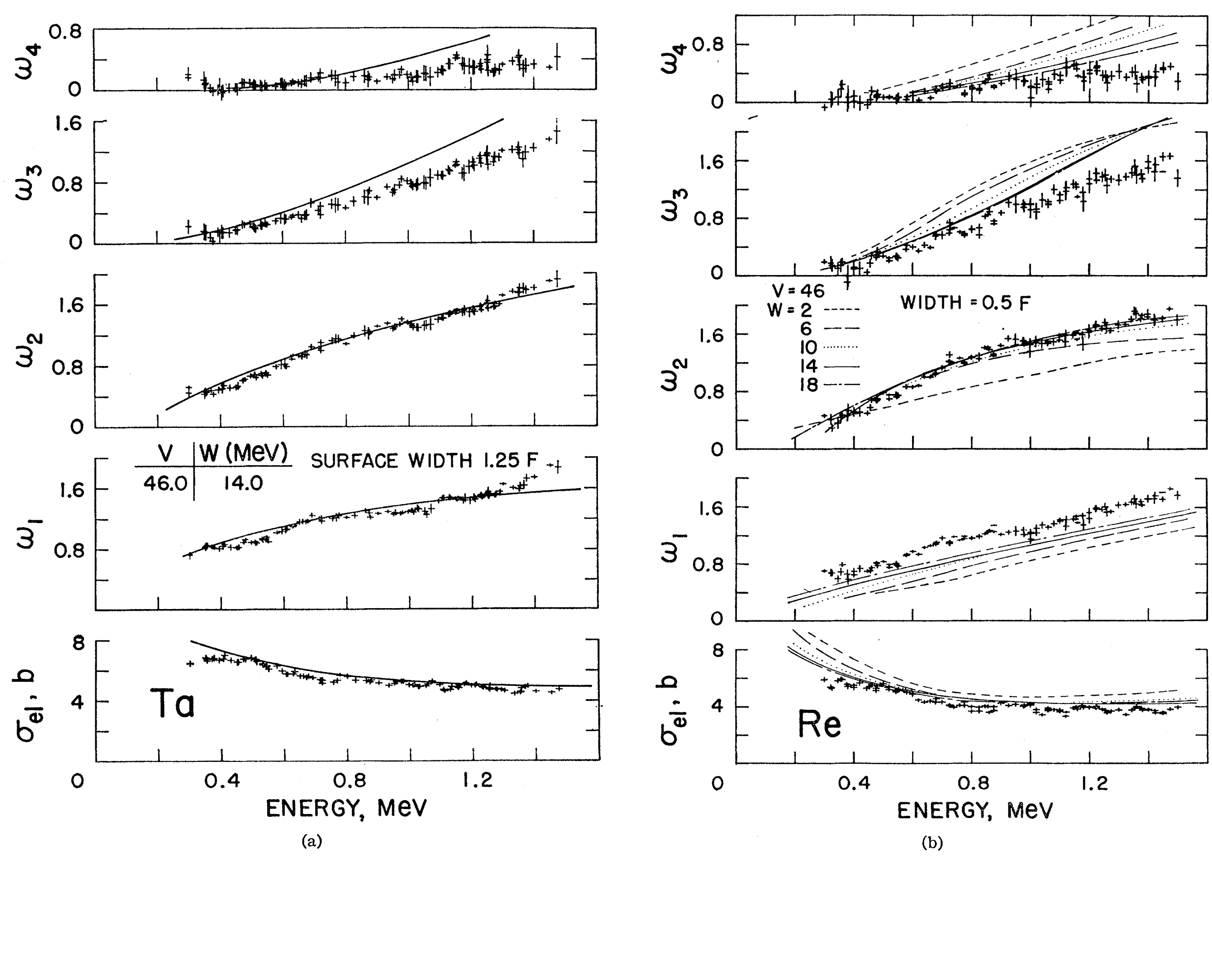

(a) (b)

the form of Eq. (1) should be extrapolated with caution beyond the measured angular interval (25° to 155°). Moreover, the experimental ω_i values may not exactly correspond to those obtained from a potential calculation as scattering angles near 0° and 180° were inaccessible to the experiment.

The experimental differential elastic scattering results for Ta, Re, and Pt, expressed in the form of Eq. (1), are given in Figs. 3(a), 3(b), and 3(c), respectively.[32] The errors associated with the measurements were difficult to quantitatively assay as the determinations were complex and often subject to appreciable human judgment. However, it was subjectively estimated that the elastic scattering cross sections were determined to $\pm 8\%$ with a 90% confidence inclusive of uncertainties in the standard cross sections of carbon and possible errors in multiple scattering and other correction factors. The illustrated ω_i errors are standard deviations derived from the least-squares fitting procedures and thus are only indicative of the quality of the fit of Eq. (1) to the individual experimental measurements. The consistency of the experimental results was good over an extended period (~4 yr).

B. Inelastic Neutron Scattering

Inelastic scattering cross sections were determined using a variety of experimental conditions chosen to emphasize particular aspects of the processes. Well-resolved inelastic neutron angular distributions were obtained for scattered neutron energies in the interval ~250 to ~1500 keV. Scattered neutrons with energies of <250 keV were qualitatively observed, but the quantitative magnitudes of the respective cross sections were uncertain due to rapid variations in the neutron detector sensitivities with neutron energy. For this reason, scattering cross sections were not quantitatively determined for scattered neutron energies of $\lesssim$250 keV. The experimental resolution was not sufficient to separate all inelastically scattered neutron groups. Closely spaced groups were occasionally observed as scattering from a single "average" state. Thus inelastic scattering cross sections are here reported for the excitation of separate states and/or combinations of states in the elemental material as is pertinent to the particular measurements and experimental resolutions.

A few of the observed inelastic differential angular distributions tended toward forward scattering. An

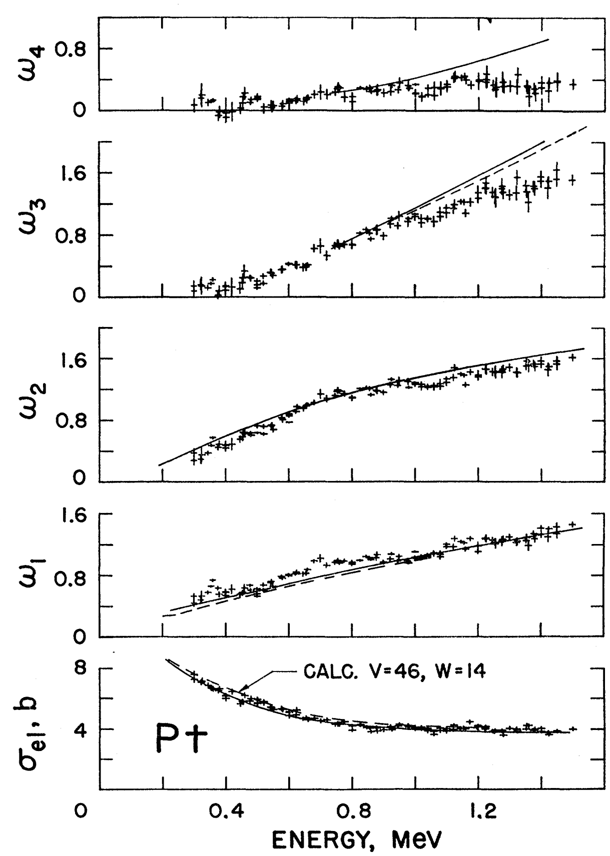

(c)

FIG. 3. (a) Differential elastic scattering cross sections of Ta expressed as Legendre expansions in the form of Eq. (1). The solid curves. are the result of calculations discussed in Sec. IV. The distributions are inclusive of inelastic scattering exciting the ~6-keV state in Ta. (b) Differential elastic scattering cross sections of Re. Format is that of (a). The curves indicate the results of calculations using various optical potentials, as discussed in Sec. IV. (c) Differential elastic scattering cross sections of Pt. Format is that of (a). The solid curves indicate the results of optical-model calculations (see Sec. IV) and the dashed lines correspond to the same calucations corrected for resonance width fluctuation effects.

[32] All data reported in this paper have been forwarded to Sigma Center, Brookhaven National Laboratory, in numerical form.

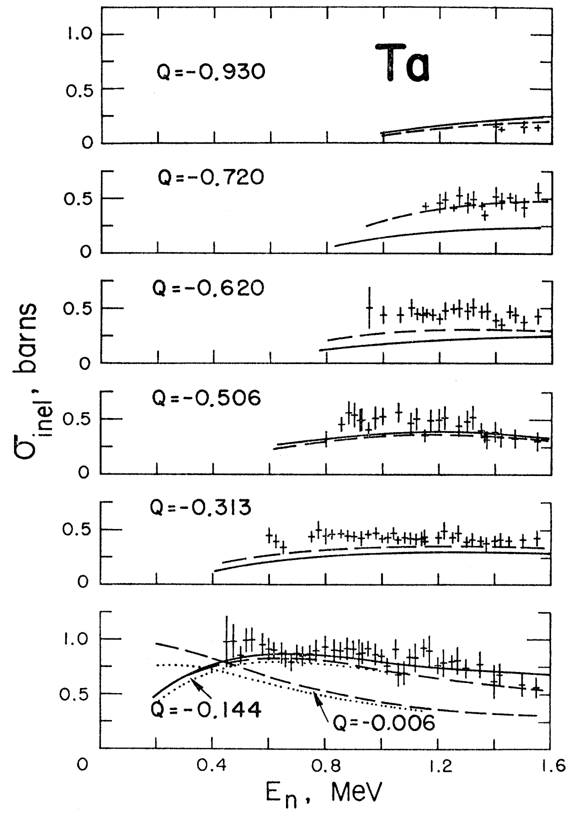

FIG. 4. Inelastic excitation cross sections of Ta. Experimental points pertaining to the respective Q values (in MeV) are shown by crosses which are indicative of estimated error in cross section and incident neutron-energy resolution. Solid lines are the results of calculations based upon the structure reported in the literature. The dashed lines were obtained using the structure "model" of Fig. 5. Dotted curves were obtained by applying fluctuation corrections to the model calculations. The lower portion of the figure indicates the calculated (not experimental) excitation of the first state at 0.006 MeV.

acute example is the excitation of the first state in Ta, as shown in Fig. 2. Most often, the observed inelastic angular distributions were essentially isotropic, as indicated for Pt in Fig. 2. The measured differential inelastic cross sections were averaged and multiplied by 4π to obtain the respective inelastic excitation cross sections. This procedure was judged to introduce $<10\%$ error in the most anisotropic cases and usually the error incurred was appreciably less than 5%. It was not always possible to determine the differential cross sections for the inelastic excitation of low-lying states at very forward angles. This was due to an inability to clearly resolve the inelastic component from the relatively intense elastic group. When this problem became serious the forward ($\lesssim 30°$) differential inelastic cross sections were not used in deducing the inelastic excitation cross sections.

Inelastic neutron groups corresponding to states in Ta at 144±10, 313±15, 506±20, 620±20, 720±20, and 930±25 keV were observed. Careful measurements, such as shown in Fig. 1, indicated the 144-keV state was a doublet with a separation of 15 to 22 keV. Qualitatively, the excitation of the lower energy state of the doublet was ~1.6 times more intense than that of the higher energy state. The observation of the energy and excitation of the state at 506 keV was complicated by the presence of the second group of neutrons from the $Li^7(p,n)Be^{7*}$ source reaction elastically scattered from the sample. The measured values were corrected for contributions due to this "second elastic" component.[28] Inelastic scattering of this second source component could have made small contributions to other observed inelastic processes. Such perturbations were assayed and found to be small; therefore no corrections were made. The measured cross sections for the inelastic excitation of the above states in Ta are shown in Fig. 4. The excited structure of Ta derived from these experiments is compared with that reported in the literature in Fig. 5.[21] The excited-state energies were determined using the time scale calibrations and reference reactions such as the inelastic excitation of the well-established 846-keV state in Fe^{56}.[21] It was felt that the energies of the excited states were conservatively determined to the specified precisions.

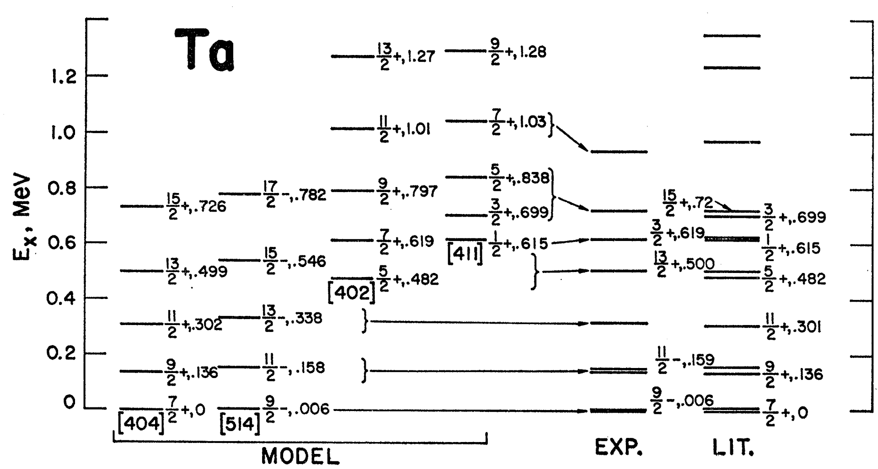

FIG. 5. Experimentally observed structure in Ta (center) is compared with that reported in the literature (right) and that of model discussed in Sec. IV (Ref. 21).

Inelastic scattering from Re was observed corresponding to the excitation of states at 132±10, 219±15, 313±15, 387±18, 518±20, 637±20, 767±25, 865±25, 963±25, 1060±25, and 1135±25 keV. The respective measured excitation cross sections are shown in Fig. 6. The observed structure is compared with that reported in the literature in Fig. 7.[21] There was some indication that the "state" at 132 keV was complex. The remarks pertaining to the measurement of the 506-keV state in Ta, above, apply to observation of the 518-keV state in Re.

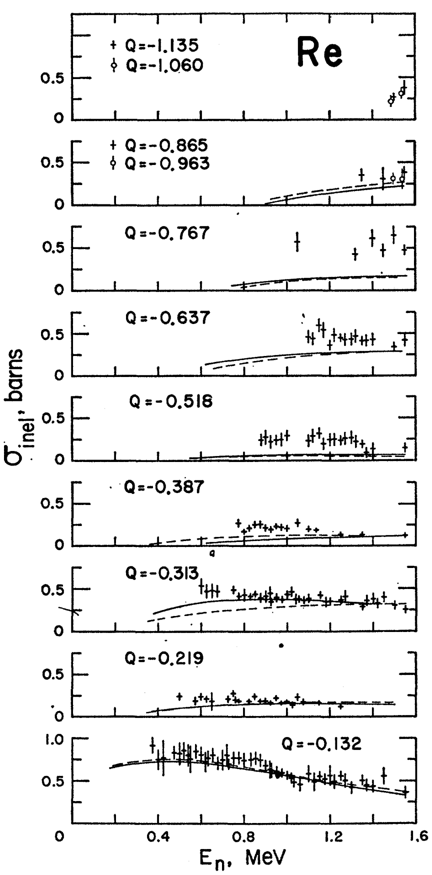

FIG. 6. Measured inelastic excitation cross sections of Re. The data points indicate the measured quantities for the respective reaction Q values (in MeV). The curves represent the results of calculations extending through the excitation of the 865-keV state as described in Sec. IV of the text.

Inelastic neutron groups observed as a result of scattering from Pt corresponded to excitation of states at 130±20, 214±20, 348±15, 420±15, 620±20, 719±15, 838±25, and 935±20 keV. The experiments indicated that "states" at 130 and 214 keV were complex, the former consisting of two major components having a separation of ~25 keV. In those cases where the 348- and 420-keV and the 620- and 719-keV states were not fully resolved, a collective cross section for an average "state" at ~360 and ~655 keV were de-

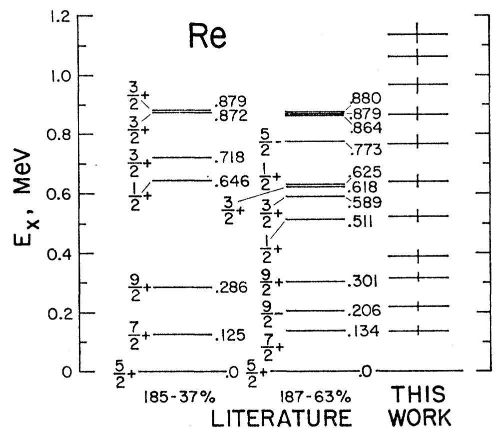

FIG. 7. A comparison of the excited structure of Re observed in this work with that reported in the literature (Ref. 21).

termined. The measured inelastic excitation cross sections for the above states in Pt are shown in Fig. 8 and the observed excited structure compared with that reported in the literature in Fig. 9.[21]

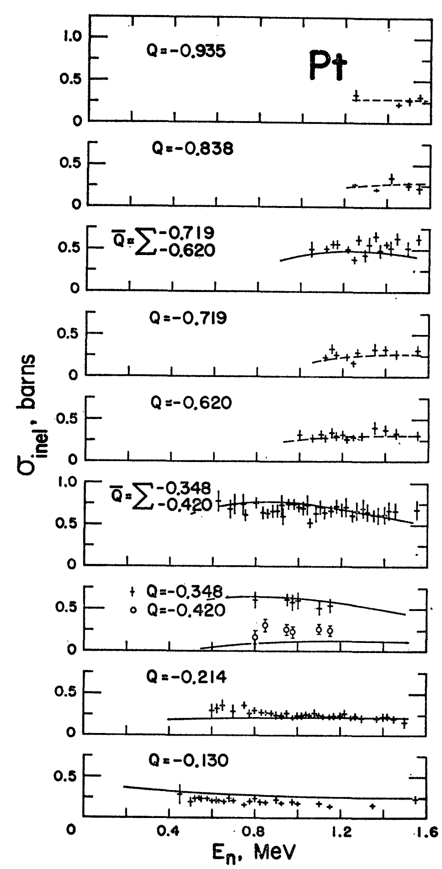

FIG. 8. Inelastic excitation cross sections of Pt. Crosses indicate the experimental results for the respective reaction Q values (in MeV). The solid curves are representative of calculation (see Sec. IV), dashed curves are "eye guides."

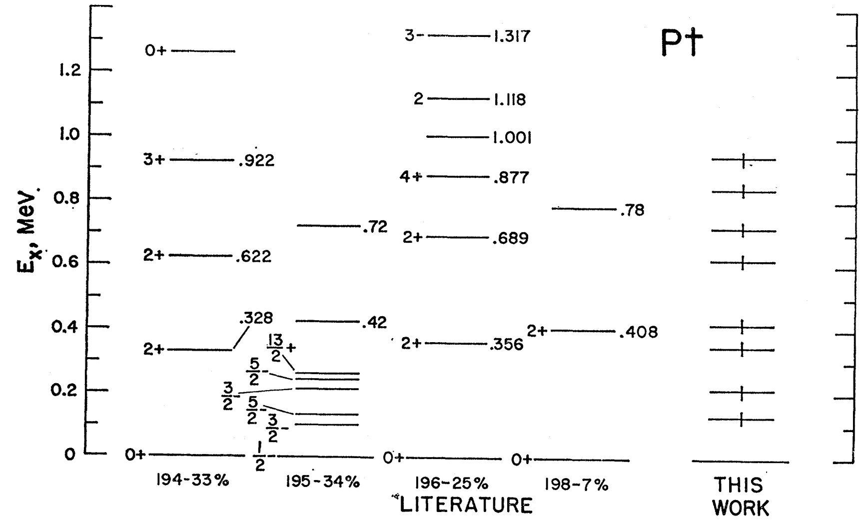

FIG. 9. A comparison of the structure of Pt derived from this work with that reported in the literature (Ref. 21).

The errors in excitation cross sections given in Figs. 4, 6, and 8 are "best judgments" of the standard deviations of the respective quantities inclusive of estimated uncertainties in the "standard" elastic scattering cross sections of carbon.[2] The determination of such errors was, of necessity, a subjective matter as the evaluation of the primary experimental information required appreciable human judgment, particularly with regard to the effect of experimental resolution.

C. Total Neutron Cross Sections

A cursory inspection of the preliminary results of this work and of the reported total cross sections and total scattering cross sections indicated a disagreement with the published total cross sections of Ta.[33] Only limited pertinent Re total cross-section information was found in the literature.[33,34] These conflicting and/or sparse experimental results stimulated the present investigation of total neutron cross sections of Re and Ta. The results are shown in Fig. 10. The experimental energy resolutions were $\lesssim 2$ keV (Ta) and ~ 5 keV (Re). The statistical standard deviations of the cross sections were 1 to 3%. During the measurements the fidelity of the apparatus was verified by determining the well-known total neutron cross section of carbon.[2,33,35]

IV. DISCUSSION

A. Experimental Comparisons

The Ta elastic scattering results of the present work can be compared with previously reported experimental values at incident energies of ~ 1.0 MeV, as shown in Fig. 11.[3,8,11] The agreement between measured values is good except near 90°, where the present work tends to result in smaller cross sections than previously reported. This discrepancy cannot entirely be explained by differing scattered neutron resolutions. Variations in the measured values near 90° should be particularly evident in the coefficients of the P_2 and P_4 terms of the Legendre expansions of the angular distributions. This was not evident when the present results for Ta and Pt were compared with the total neutron scattering distributions of Langsdorf *et al.*[2] Particularly in the case of scattering from Ta near 1.0 MeV the Langsdorf results, when corrected for inelastic scattering contributions, yielded ω_2 and ω_4 coefficients essentially identical to those obtained in the present elastic scattering studies. Moreover, the directly measured total cross sections of Ta as determined in this work (Fig. 10) are very similar to the total scattering cross section reported by Langsdorf *et al.* The total scattering cross sections of both Ta and Pt obtained by summing the present elastic and inelastic results differ by only a few percent from the Langsdorf values. The measured total cross sections and scattering cross sections of Re determined in this work are consistent. Previously reported Re cross sections are too fragmentary to permit a reasonable quantitative comparison with past work.[33]

A few direct measurements of inelastic scattering from Ta have been reported. Preliminary studies by the present authors are in substantial agreement with the results given here.[4] There are only minor differences between the past and the present work near an excitation energy of *950* keV, where the later detailed results did not confirm a doublet structure initially reported.[36] Garber and Shrader have measured the differential cross sections for the excitation of the *144* and *313* keV states at an incident neutron energy of ~ 700 keV.[7]

[33] *Brookhaven National Laboratory Report No. 325*, compiled by D. J. Hughes and R. Schwartz (U. S. Government Printing Office, Washington, D. C., 1958), 2nd ed.

[34] Information contained in M. Goldberg *et al.*, [in *Brookhaven National Laboratory Report No. 325* (U. S. Government Printing Office, Washington, D. C., 1966), 2nd ed., Suppl. 2, Vol. II-C] is more definitive owing in part, to the prepublication use of data from the present experiments.

[35] J. Whalen *et al.* (private communication); see also Ref. 33 above.

[36] In subsequent portions of this paper an energy value in italics denotes a magnitude as observed in the present experiments.

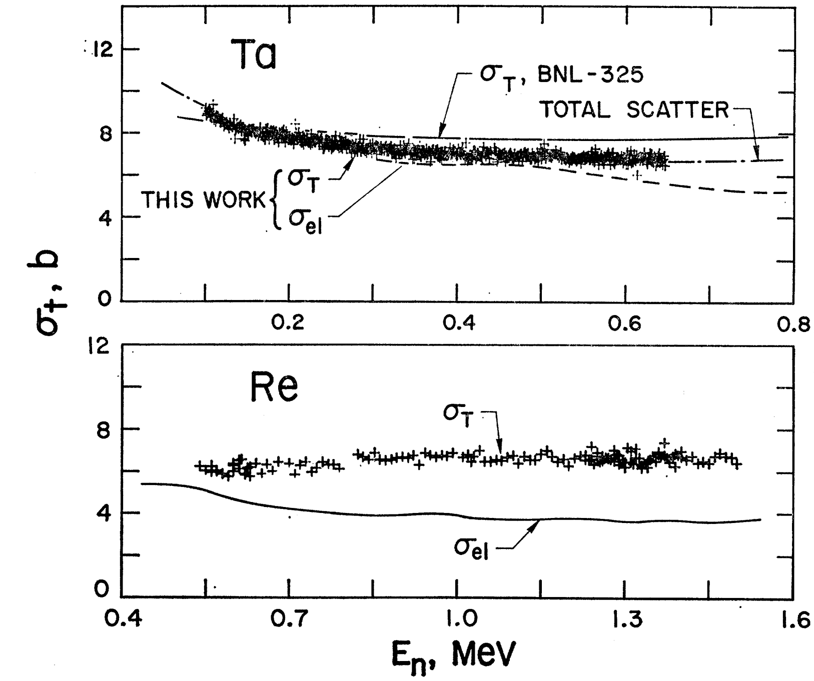

FIG. 10. The data points represent the measured total cross sections of Ta and Re. σ_{el} curves were obtained from the present work and the total scattering curve taken from Langsdorf *et al.* (Ref. 2).

Their results were somewhat larger than those given here. This could have been due to multiple scattering effects for which they made no corrections. Inelastic scattering from Ta has been studied using threshold detectors.[37] The measured values were sensitive to the setting of the detector threshold in the context of the complex inelastically scattered neutron spectrum. Perhaps for this reason the threshold detector results are in only fair agreement with those obtained in the present work.

Results of a number of studies of the $(n; n'\gamma)$ processes in Ta, Re, and Pt have been reported.[6,9,10,38] Measurements of this type are not always easy to evaluate in terms of inelastic scattering cross sections as the interpretation can depend upon a quantitative knowledge of internal conversion, branching ratios, angular distributions, and experimental factors, such as γ-ray absorption within the samples. Thus it is not surprising that inelastic scattering cross sections deduced from $(n; n'\gamma)$ studies of Ta, Re, and Pt are not always in qualitative agreement with the results of the present work.

B. Comparison with Calculation and Structure Systematics

The elements Ta, Re, and Pt are primarily constituted of the following isotopes: Ta^{181} (99%); Re^{185} (37%), Re^{187} (63%); Pt^{194} (33%), Pt^{195} (34%), Pt^{196} (25%), and Pt^{198} (7%). Scattering from these elements is complex because of the isotopic mixture and/or the complicated nuclear structure. These factors make it difficult to compare calculated elastic and inelastic neutron scattering with experimental observation. The calculational procedure followed here consisted of an initial searched for an optical potential reasonably describing the observed elastic neutron scattering, inclusive of compound-nuclear contributions, assuming the low-energy excited structure reported in the literature was valid.[18,39–41] The search was restricted to the

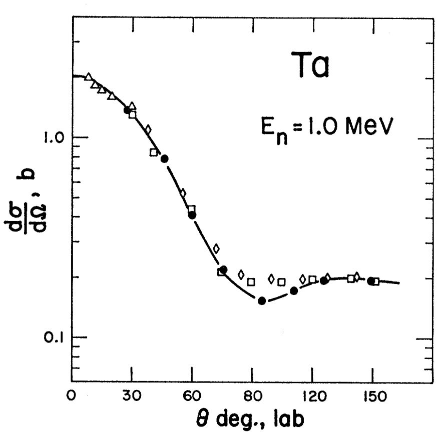

FIG. 11. Differential elastic scattering cross section of Ta at ~1.0 MeV. Cross sections obtained in this work are indicated by solid data points; △ indicate results of S. E. Darden *et al.* [Phys. Rev. **96**, A836 (1954)], □ of Ref. 3, and ◇ of Ref. 8. The curve is a fit of Eq. (1) to the data of the present experiment.

[37] N. P. Glaskov, Atomnaya Energiya, **15**, 416 (1963).
[38] L. Ya. Graudynya *et al.*, Zh. Eksperim. i Teor. Fiz. **42**, 349 (1967). [English transl.: Soviet Phys.—JETP, **15**, 240 (1962)].
[39] H. Feshbach *et al.*, Phys. Rev. **96**, 448 (1954).
[40] W. Hauser and H. Feshbach, Phys. Rev. **87**, 366 (1952).
[41] L. Wolfenstein, Phys. Rev. **82**, 690 (1951).

following spherical, local, nonenergy-dependent, and surface-absorption optical potential suggested by Moldauer[42]:

$$-Vq-iWp+V_{so}\left(\frac{h}{\mu_\pi c}\right)^2\sigma\cdot\mathbf{l}\frac{1}{r}\left(\frac{dq}{dr}\right),$$

$$q(r)=[1+\exp((r-R)/a)]^{-1}, \quad (2)$$

$$p(r)=\exp[-((r-R-c)/b)^2],$$

$$R=r_0A^{1/3}+r_1,$$

where $r_0=1.16$ F, $r_1=0.6$ F, $a=0.62$ F, and $c=0.5$ F. The potential of Eq. (2) has been shown widely valid in neutron-scattering calculations at incident neutron energies of $\lesssim 2$ MeV and it does form a convenient spherical approximation from which to attempt a description of the results of these experiments.[42] However, this spherical potential is not strictly applicable to the deformed nuclei Ta, Re, and Pt and can provide no insight into the direct interaction between the neutron and collective nuclear configurations. Such direct reaction processes are probably not large at the energies of these experiments as indicated by the near isotropy of most of the observed inelastic scattering angular distributions.

Elastic neutron-scattering angular distributions were calculated at incident energy intervals of $\lesssim 0.2$ MeV from 0.2 to 1.6 MeV, using a predetermined matrix of V and W values extending over the intervals $40\leq V\leq 50$ MeV and $2\leq W\leq 20$ MeV.[43] From this V-W space a region yielding a "good" description of the measured elastic scattering results was selected for more detailed calculation and the selection of the "best" V and W values. This selection was primarily subjective but was guided by minimum χ^2 fits to a number of the measured angular distributions, particularly at lower incident energies. χ^2 fitting of all the measured elastic distributions was not economically feasible and this fitting procedure tended to yield ambiguous V and W values at the upper extreme of the measured energy interval. Subsequent to the above procedures, resonance width fluctuation corrections were applied following the method of Moldauer.[43,44] Generally, these corrections did not appreciably alter the initial results [see Fig. 3(c), for example].

After a "satisfactory" description of the measured elastic scattering had been achieved, the inelastic scattering cross sections were calculated using the Hauser-Feshbach formula.[40,41] The excited structure reported in the literature was modified with respect to energies, spins, and parities, and additions or deletions made in an attempt to obtain a reasonable description of the experimental inelastic results. These modifications were guided by and related to the theoretical understanding of excited states in deformed nuclei and the comparison of calculation and experiment provided an insight into the nature of this structure.[20,45]

The results obtained using the above procedures are outlined in the following by element. They are most detailed for the mono-isotopic element Ta and become progressively less definitive for the more isotopically complex elements Re and then Pt.

1. Tantalum

$_{73}Ta^{181}$ has been extensively studied using Coulomb excitation methods and by observing the radioactive decay of both Hf^{181} and W^{181}.[21] The low-energy excited structure is attributed to single-particle states and their associated rotational bands.[45] Vibrational states are apparently not contributing factors at excitation energies available in the present experiments. The single-particle structure is described by the calculations of Mottelson and Nilsson.[20] Assuming a deformation of $\delta\sim 0.3$ these calculations attribute to the 73rd proton a $\frac{9}{2}-[514]$ or $\frac{5}{2}+[402]$ state. However, the $\frac{7}{2}+[404]$ state is energetically similar to the $\frac{9}{2}-[514]$ state and the pairing energy can result in a ground state of $\frac{7}{2}+[404]$ in accord with observation. The first excited state is then $\frac{9}{2}-[514]$ and is identified with the $\sim$6-keV state not resolved in the present experiments. The next single-particle state should then be $\frac{5}{2}+[402]$ and is reported at an energy of 482 keV. A $\frac{1}{2}+[411]$ state with a $(\frac{1}{2}+)$ $(\frac{7}{2}+)^2$ $(\frac{9}{2}-)^2$ single-particle configuration is reported at an energy of 615 keV. As illustrated in Fig. 5, the above single-particle states appear to have associated rotational bands.

Initial elastic scattering calculations were made with the surface absorption width b held constant at 0.5 F and V and W varying. The calculated results were not particularly descriptive of either the measured total elastic scattering cross sections, the total cross sections, or the observed elastic angular distributions. Small real potentials ($V\sim 42$ MeV) resulted in inelastic cross sections in fair agreement with observed values but were particularly poor in describing the experimental elastic scattering cross sections.

In an attempt to improve the description of scattering from Ta, the Gaussian surface absorption width of the potential of Eq. (2) was made, in addition to V and W, a variable. In this manner a reasonable agreement with experiment was achieved, with $V=46$ MeV, $W=14$ MeV, and $b=1.25$ F. These calculated results are indicated by the solid curves in Fig 3(a), and are in reasonable agreement with the experimental elastic scattering, total neutron cross sections and, at incident neutron energies of $\lesssim 1.2$ MeV, with the elastic angular

[42] P. A. Moldauer, Nucl. Phys. **47**, 65 (1963).
[43] The following calculational computer codes were employed; (a) NEARREX [P. Moldauer *et al.*, Argonne National Laboratory Report No. ANL-6978, 1964 (unpublished)]; (b) ABACUS-2, [E. Auerbach, Brookhaven National Laboratory Report No. BNL-6562 1962 (unpublished)].
[44] P. A. Moldauer, Rev. Mod. Phys. **36**, 1079 (1964).
[45] M. A. Preston, *Physics of the Nucleus* (Addison-Wesley Publishing Co., Inc., Reading, Mass., 1962), Chap. 10.

distributions. Above ~1.2 MeV, calculation tends to deviate from experiment particularly with respect to $\omega_3, \omega_4, \omega_5$. The potential of Eq. (2) with these parameters was judged a reasonable "spherical" approximation for calculating neutron scattering from the deformed nucleus Ta and resulted in a better agreement with experiment than reported with some other spherical potentials.[19] The potential differs from that generally proposed by Moldauer only in the Gaussian absorption width of 1.25 F, as compared to the value of 0.5 F found applicable to lighter and spherical nuclei.[42] It is tempting to associate this difference with the large deformation of Ta^{181}.

Using level structure reported in the literature[21] (Fig. 5) and the above potential, the inelastic excitation cross sections of Ta were calculated with results indicated by the solid curves of Fig. 4. The calculated excitation of the unresolved $\frac{9}{2}-$ state at ~6 keV was large and was included with the elastic component in making comparisons with measured elastic scattering. The calculated cross section for the excitation of the observed composite *144*-keV state ($\frac{11}{2}-$, $\frac{9}{2}+$) was similar to the measured value and, indeed, the calculated ratio of the excitation of the $\frac{9}{2}+$ to that of the $\frac{11}{2}-$ state was ~1.9, qualitatively in agreement with the experimental estimate of ~1.6. Calculated values were slightly lower than the experimentally observed excitation of both the *313*-keV ($\frac{11}{2}+$) state and the *506*-keV ($\frac{13}{2}+$, $\frac{5}{2}+$) state. Calculated cross sections for the excitation of the *620*-keV ($\frac{1}{2}+$, $\frac{3}{2}+$) and the *720*-keV ($\frac{15}{2}+$, $\frac{3}{2}+$) states were appreciably lower than the experimental values. Uncertain assignments of ($\frac{11}{2}+$, $\frac{7}{2}+$) were used in calculating the excitation of the *930*-keV state and, as a result, the computed values are speculative. Width fluctuation corrections (Q of Ref. 44=0.5) did not appreciably alter the calculated cross sections (see dotted curves of Fig. 4). It is as would be expected from the number of available exit channels.[44]

The differences between the calculated and observed excitations of the *620*- and *720*-keV states could have been attributed to uncertainty and/or incompleteness in the pertinent reported structure employed in the calculations. As an alternative to the published structure a single-particle rotational model (left of Fig. 5) was constructed from the predictions of Mottelson and Nilsson and the energetics of the observed low-energy structure retaining only such states as could be excited by neutrons of $l \lesssim 4$.[20,45] The first two rotational sequences of the model, based upon [404] and [514], were well established from a number of measurements.[21] Only the initial states ($\frac{5}{2}+$[402] and $\frac{1}{2}+$[411]) of the two subsequent sequences were experimentally defined.[21] It was assumed that the reported states at 619 and 699 keV were $\frac{7}{2}+$ and $\frac{3}{2}+$, respectively, and the second members of the rotational sequences. With this premise the remaining structure of the model, shown in Fig. 5, followed. The energetics of the simple model were not expected to accurately agree with experiment as no cognizance was taken of perturbing effects, such as Coriolis mixing of internal motions and rotations, but the model did form a qualitative basis for the calculation and the assay of observed excited structure.

Results of calculations carried out using the model are indicated by the dashed curves of Fig. 4. These results are in better agreement with experiment than those obtained using the reported structure (solid curves of Fig. 4), particularly for excitations in the range 600 to 800 keV. This improved agreement is principally due to the [402] and [411] sequences of the model, which are consistent with previously reported structure information with the exception of $\log ft$ values obtained from studies of a weak β-ray transition (~4%) from Hf^{181}.[21] The instrumental resolution and available energy range of the present experiments was not sufficient to permit a more critical assay of the model or alternative structure concepts. However, results of the present experiment and calculations based upon the reported structure were clearly inconsistent, indicating that a revision in the reported structure of Ta was warranted.

2. Rhenium

The initial calculations of elastic and the inelastic neutron scattering from Re utilized the reported level structure of Re^{185} and Re^{187} (Fig. 7) and the potential of Eq. (2).[21] The surface absorption width was fixed at $b=0.5$ F and V and W varied to obtain the "best" description of experiment. Results of calculations employing a real potential $V=46$ MeV and imaginary potentials $2 \leq W \leq 18$ MeV are compared with measured elastic scattering cross sections in Fig. 3(b). Parameter values $V=46$ MeV and $W=14$ MeV were accepted as providing a reasonable description of elastic scattering and total neutron cross sections of Re although the calculated elastic angular distributions were in only fair agreement with experiment. Attempts to improve the agreement with experiment by allowing potential parameters (other than V and W) to vary were not successful. In particular, a value of $b=1.25$ F, as selected for Ta above, resulted in poor agreement with experiment at incident neutron energies of $\lesssim 700$ keV. The difference in the potential surface absorption width selected for Ta and for Re may reflect the smaller distortion of Re ($\delta \sim 0.2$) as compared to Ta ($\delta \sim 0.3$).[1]

The low-energy excited structure of the 185 and 187 isotopes of Re can be described in terms of single-particle and associated rotational states, with γ-vibrational states at excitation energies above ~600 keV.[20,21,45] Assuming strong pairing, the unified mode predicts a ground state of $\frac{5}{2}+$[402] with the particle configuration $(\frac{7}{2}+)^2$ $(\frac{5}{2}+)$ $(\frac{9}{2}-)^2$, in accord with observation. The next single-particle configuration is $(\frac{7}{2}+)^2$ $(\frac{5}{2}+)^2$ $(\frac{9}{2}-)$, corresponding to the reported $\frac{9}{2}-$[514] states in Re^{187} at 205 keV and observed as a *219*-keV state in the present experiments. The first and second excited states in the ground-state rotational sequence of both Re isotopes ($\frac{7}{2}+$, $\frac{9}{2}+$) have been observed in Coulomb excitation experiments and were evident as states at *132* and *313* keV in the present work.[21,22] The theoretically predicted $\frac{9}{2}-$ single-particle state in Re^{185} presents an enigma. It has not been reported in Coulomb excitation studies (which would not have been sensitive to its presence) yet its analog is evident in Re^{183} (496 keV) and Re^{187} (206 keV). The state in Re observed in the present work at *387* keV energetically corresponds to the predicted and heretofore missing $\frac{9}{2}-$ single-particle state in Re^{185}.

Above excitation energies of $\sim$500 keV the structures in Re^{185} and Re^{187} are complex and uncertain and the resolution of the present work limits the experimental information. The *518*-keV state observed in the present work was attributed to the reported $\frac{1}{2}+$ (511-keV) state in Re^{187}; the *637*-keV state to a composite of $\frac{1}{2}+$ and $\frac{3}{2}+$ states in both isotopes; the *767*-keV state to $\frac{3}{2}+$ (Re^{185}) and $\frac{5}{2}-$ (Re^{187}) states; the *865*-keV state to a complex of levels in both isotopes; and the structure origin of observed states at *963*, *1060*, and *1135* keV remained obscure.

The inelastic excitation cross sections of Re were calculated using the above "best" potential and the reported excited structure with the addition of a $\frac{9}{2}-$ state at *387* keV in the Re^{185} isotope. The calculated results, indicated by the solid curves in Fig. 6, reasonably described the excitation of states with energies of $\lesssim$500 keV. However, the agreement with experiment deteriorated as the excitation energy extended above 500 keV. The discrepancy between the calculated and measured excitation of the states at *767*, *518*, and *637* keV cast doubt on the validity and/or completeness of the reported structure in this energy region. The inversion of the parities of the $\frac{9}{2}-$ states on Re^{185} was considered. The results of calculations assuming assignments $\frac{9}{2}+$ (*387* keV) and $\frac{9}{2}-$ (*286* keV) did not significantly improve the agreement with experiment, as is illustrated by the dashed curves in Fig. 6, nor was such an inversion compatible with the results of a number of Coulomb excitation experiments. It was thus concluded that the *387*-keV state observed in the present experiments was likely the predicted $\frac{9}{2}-$[514] single-particle state in Re^{185}.[46]

3. *Platinum*

Pt was the most isotopically complex of the elements studied and the computation of cross sections would have been extensive if carried out by isotope. In order to avoid these complexities, the present calculations were based upon a simplified model element consisting of Pt^{194} (66%) and Pt^{195} (34%). This model reasonably described rotational ($K=0$) and the γ-vibrational ($K=2$) states of the even isotopes of Pt in the energy range of interest and accurately represented the odd isotope of the element, Pt^{195}. Using this model, the published structure of Pt^{194} and Pt^{195}, and the potential of Eq. (2), a good description of elastic scattering was obtained with a real potential magnitude $V=46$ MeV, an imaginary potential $W=14$ MeV, and an absorption width of $b=0.5$ F, as indicated by the solid curves in Fig. 3(c). This agreement between calculation and experiment was superior to that obtained for either Re or Ta, possibly as a result of the relatively small deformation of Pt ($\delta\sim0.15$).[1] The effect of resonance width fluctuations was assayed and found small as indicated by the dashed lines of Fig. 3(c).

The observed inelastic excitation of states at *130* and *214* keV was attributed to pairs and triplets of states in Pt^{195} as illustrated in Fig. 9. The observed *348*-keV state was believed a composite of contributions from 2+ states in the even isotopes and the *420*-keV state was attributed entirely to a 420-keV $\frac{5}{2}+$ level in Pt^{195}. No quantitative correlation with reported structure was attempted at excitations above $\sim$600 keV. Qualitatively, the observed states at *620* and *719* keV are attributed to 2+ γ-vibration states in the even isotopes and a $\frac{7}{2}+$ state in Pt^{195}.

The inelastic excitation cross sections were calculated using the above potential and the model with the results indicated by the solid curves of Fig. 8. The agreement between calculation and experiment was reasonable at excitation energies where the model was a suitable approximation of the complex structure of the natural element.

V. SUMMARY

The present experiments extended the knowledge of elastic and inelastic neutron scattering and total cross sections of Ta, Re, and Pt at incident neutron energies of $\lesssim$1.5 MeV. The measured results were reasonably described by calculations based upon a local, energy-independent optical potential and the theory of average compound-nucleus cross sections. The calculations demonstrated the qualitative applicability of a well-chosen spherical, surface absorption, optical potential for the interpolation and extrapolation of measured scattering cross sections over a region of large and rapidly changing deformation. Comparison with experiment suggested a proportionality between the strength of the surface absorption and the degree of deformation. Resonance width fluctuation effects were examined and found to be small. Uncertainties in calculated inelastic scattering cross sections, particularly at excitations $\gtrsim$500 keV, tended to be more the result of inadequate knowledge of excited nuclear structure than of deficiencies in the potential employed.

[46] Since completion of this work and preparation of this manuscript extensive studies of resonance florescence in Re^{187} have been reported [(H. Langhoff, Phys. Rev. **159**, 4 (1967); **159**, 1033 (1967)]. These results do indicate complex structure at excitations >500 keV due primarily to γ-vibrational states. The spins and parities proposed from this recent work differ from those previously reported. However, these changes in the structure of Re^{187} are not alone sufficient to account for the discrepancies between calculation and experiment noted above.

The derivation of structure information from the measurements was restricted by experimental resolutions and sensitivities and by the isotopic complexity of the natural elements employed in the work. Despite these restrictions the experiments indicated that there were omissions and/or inappropriate spin and parity assignments in the reported low-energy excited structure of both Ta and Re. Revisions of the excited structure of Ta consistent with the unified model and experimental observation were proposed. Modifications of and additions to the reported structure of Re were suggested by the experimental results inclusive of a specific state attributed to a predicted single-particle configuration in Re^{185}.

ACKNOWLEDGMENTS

The authors are appreciative of assistance rendered by a number of members of the Applied Nuclear Physics Section, Reactor Physics Division, Argonne National Laboratory.

PHYSICAL REVIEW VOLUME 168, NUMBER 4 20 APRIL 1968

$^{90,92,94}Zr(p,p')$ Reactions at 12.7 MeV*

J. K. Dickens, E. Eichler, and G. R. Satchler
Oak Ridge National Laboratory, Oak Ridge, Tennessee
(Received 22 November 1967)

The elastic and inelastic scattering of 12.7-MeV protons from $^{90,92,94}Zr$ has been studied. Angular distributions for the elastic and 40 inelastic groups were measured. An optical-model analysis of the elastic scattering was performed. The inelastic scattering was interpreted, using the usual "collective"-model interaction and the distorted-wave approximation. Multipolarities L were assigned where possible, and strength parameters β_L were deduced. The inelastic scattering to some states was also compared with the predictions of the shell model, using a simple two-body interaction of Yukawa type and including the effects of core polarization. Reasonable agreement was obtained, although the angular distributions for the 0^+ and 3^- excitations imply that a more sophisticated effective interaction is required.

I. INTRODUCTION

THE excitation of levels in ^{90}Zr by 18.8-MeV protons[1] and in $^{92,94}Zr$ by 19.4-MeV protons[2] has been reported recently and the measurements were interpreted in terms of a microscopic description of the interaction, using shell-model wave functions for the target nuclei.[3,4] The apparent success of this analysis lent additional interest to obtaining similar data at other energies. Partly for this reason, measurements on these nuclei were also made using 12.7-MeV protons. In addition, better energy resolution was obtained than at the higher energies and a few new transitions were detected. In particular, angular distributions were obtained for the excitation of the lowest 0^+ excited state in each isotope, and these are of considerable theoretical interest.

Inelastic scattering from these isotopes provides a useful testing ground for the microscopic description of the interaction because often the states of low excitation may be identified with simple shell-model configurations involving very few valence nucleons.[5] The model takes a two-body "effective" interaction between the projectile and each target nucleon. The earlier analyses[3] were directed toward determining the parameters of this effective interaction. Since then it has been realized that, in addition to the direct interaction between the projectile and the valence nucleons of the target, there are important contributions due to virtual excitations of the core nucleons.[6] (The same contributions give rise to the need to use effective charges for the valence nucleons in electromagnetic transitions.) The parameters for these core polarization terms are often not known. Hence there is a corresponding uncertainty in deducing the parameters of the direct coupling between projectile and valence nucleon. For this reason, less was learned from the data to be reported here than had been hoped originally. Nonetheless, the data are an important check for any further developments of the theory.

Since this work was completed, measurements of the scattering of 14.5-MeV protons by $^{90,92}Zr$ have been reported.[7] The measurements are not as extensive as

* Research sponsored by the U. S. Atomic Energy Commission under contract with Union Carbide Corporation.
[1] W. S. Gray, R. A. Kenefick, J. J. Kraushaar, and G. R. Satchler, Phys. Rev. **142**, 735 (1966).
[2] M. M. Strautberg and J. J. Kraushaar, Phys. Rev. **151**, 969 (1966).
[3] M. B. Johnson, L. W. Owen, and G. R. Satchler, Phys. Rev. **142**, 748 (1966); G. R. Satchler, Nucl. Phys. **A95**, 1 (1967).
[4] H. O. Funsten, N. R. Roberson, and E. Rost, Phys. Rev. **134**, B117 (1964); V. A. Madsen and W. Tobocman, *ibid.* **139**, B864 (1965); N. K. Glendenning and M. Veneroni, *ibid.* **144**, 739 (1966); G. R. Satchler, Nucl. Phys. **77**, 481 (1966); V. A. Madsen, *ibid.* **80**, 177 (1966).
[5] B. F. Bayman, A. S. Reiner, and R. K. Sheline, Phys. Rev. **115**, 1627 (1959); I. Talmi and I. Unna, Nucl. Phys. **19**, 225 (1960); I. Talmi, Phys. Rev. **126**, 2116 (1962).
[6] W. G. Love and G. R. Satchler, Nucl. Phys. **A92**, 11 (1967).
[7] K. Matsuda, H. Nakamura, I. Nonaka, H. Taketani, T. Wada, Y. Awaya, and M. Koike, J. Phys. Soc. Japan **22**, 1311 (1967).